

Excitation of high-radial-order Laguerre-Gaussian modes in a solid-state laser using lower-loss digitally controlled amplitude mask

This content has been downloaded from IOPscience. Please scroll down to see the full text.

Download details:

IP Address: 146.64.81.115

This content was downloaded on 25/07/2017 at 15:39

Manuscript version: Accepted Manuscript

Bell et al

To cite this article before publication: Bell et al, 2017, J. Opt., at press:

<https://doi.org/10.1088/2040-8986/aa81f9>

This Accepted Manuscript is: © 2017 IOP Publishing Ltd

During the embargo period (the 12 month period from the publication of the Version of Record of this article), the Accepted Manuscript is fully protected by copyright and cannot be reused or reposted elsewhere.

As the Version of Record of this article is going to be / has been published on a subscription basis, this Accepted Manuscript is available for reuse under a CC BY-NC-ND 3.0 licence after the 12 month embargo period.

After the embargo period, everyone is permitted to copy and redistribute this article for non-commercial purposes only, provided that they adhere to all the terms of the licence

<https://creativecommons.org/licences/by-nc-nd/3.0>

Although reasonable endeavours have been taken to obtain all necessary permissions from third parties to include their copyrighted content within this article, their full citation and copyright line may not be present in this Accepted Manuscript version. Before using any content from this article, please refer to the Version of Record on IOPscience once published for full citation and copyright details, as permission will likely be required. All third party content is fully copyright protected, unless specifically stated otherwise in the figure caption in the Version of Record.

When available, you can view the Version of Record for this article at:

<http://iopscience.iop.org/article/10.1088/2040-8986/aa81f9>

Excitation of high-radial-order Laguerre-Gaussian modes in a solid-state laser using lower-loss digitally controlled amplitude mask

T Bell^{1,2}, A Hasnaoui³, K Ait-Ameur⁴, S Ngcobo¹

¹National Laser Centre, Council for Scientific and Industrial Research, Meiring Naude Rd, Pretoria 0001, South Africa

²School of Chemistry and Physics, University of KwaZulu-Natal, King George V Ave, Durban 4041, South Africa

³Laboratoire Sciences Nucleaires et Interaction Rayonnement Matiere (SNIRM), Faculte de physique, USTHB, BP n°32, El Alia, Algiers 16111, Algeria

⁴Centre de recherche sur les Ions, les Materiaux et la Photonique (CIMAP) UMR 6252 CEA-CNRS-ENSICAEN-University of Caen, 6 Bd. Marechal Juin, 14050 Caen, France

E-mail: sngcobo@csir.co.za

20 May 2017

Abstract. In this paper, we experimentally demonstrate selective excitation of high-radial-order Laguerre-Gaussian (LG_p or $LG_{p,0}$) modes with radial-order, $p = 1 - 4$ and azimuthal-order, $l = 0$, using a diode-pump solid-state laser (DPSSL) that is digitally controlled using Spatial Light Modulator (SLM). We encoded amplitude mask containing p -absorbing rings, of various incompleteness (segmented), on grey-scale computer generated digital holograms (CGDH), and displayed them on an SLM, that acted as an end mirror of the diode-pumped solid-state digital laser (DPSSDL). The various incomplete (α) p -absorbing rings were digitally encoded to match the zero intensity nulls of the desired LG_p mode. We illustrate that the creation of LG_p , for $p = 1$ to $p = 4$, only requires an incomplete circular p -absorbing ring that have a completeness of $\approx 37.5\%$, which makes the DPSSL resonator to have the lower pump threshold power, while maintaining the same laser characteristics (such as beam propagation properties).

PACS numbers: 42.40, 42.55, 42.60

Keywords: solid-state lasers, laser resonators, spatial light modulators, laser beam characterization

Submitted to: *Journal of Optics*

1
2
3 *lower-loss digitally controlled amplitude mask* 2
4

5 **1. Introduction**

6
7 High-order Laguerre-Gaussian ($LG_{p,l}$) beams are used in many applications such as
8 in industry, medicine, military, communication, microscopy and sensing [1, 2, 3, 4].
9 Applications such optical trapping [5], which are also termed optical tweezers, have
10 been shown that they would be inconceivable without higher-order Laguerre-Gaussian
11 ($LG_{p,l}$) beams. Especially those that only contains the azimuthal order, l , component
12 as they can transfer orbital momentum (OM) to a trapped particle (this is mainly used
13 for manipulating biological cells). By creating a vortex field around the particle thereby
14 “forcing” the particle to rotate around the optical axis of the beam and trapping the
15 cell [6]. The interest over the years for $LG_{0,l}$ beams that have only the azimuthal index
16 have even lead to the optical tweezers to be known as optical vortices [7].
17

18
19 The current demand for high brightness lasers, especially in military and
20 applications that require high brightness lasers, has sparked an interest to study further
21 high order LG beams, especially those that have only the radial order, p , index. The
22 notion is to intra-cavity generate LG_p mode to be a fundamental mode that will have
23 high energy [8]. Over the years it has been shown that LG_p modes can be created using
24 extra-cavity and intra-cavity methods [9, 10, 11]. The major disadvantage of LG_p modes
25 in many applications has been using the laser that produces the fundamental Gaussian
26 beam.
27

28
29 In this article, we utilised a new technology called the diode-pumped solid-state
30 digital laser (DPSSDL) that was recently invented at the Council for Scientific and
31 Industrial Research in South Africa (CSIR), Pretoria, Republic of South Africa [11].
32 We used this technology to generate high-order Laguerre-Gaussian modes (LG_p) of the
33 radial index, p , and zero azimuthal order index, l . It has been already shown that these
34 modes can be generated by inserting of a mask made-up of p -absorbing rings having
35 a radius coinciding with the zeros of the desired LG_p mode within the cavity [12].
36 However, doing that introduces supplementary losses and consequently increases the
37 laser threshold. In this article, we will show that it is possible to force the fundamental
38 mode of the laser to be a single high-order LG_p mode by using incomplete absorbing
39 rings allowing the reduction of inserting losses [13, 14]. It is worthwhile to recall that
40 an LG_p beam is made up of a central peak surrounded by p -rings of light separated by a
41 p -zeros of intensity. The laser resonator that we opted to use was a diode-end-pumped
42 system due to the ease of controlling the pump spot size, the wavelength of the pump,
43 the divergence and incident angle of the pump beam onto the gain medium [15, 16, 17].
44

45 Forcing the fundamental mode to be an LG_p mode can offer some advantages:
46

- 47 • An improved energy extraction from the laser medium due to a great lateral extent
48 compared to the usual Gaussian beam. The LG_p mode can be transformed in the
49 focal plane of a lens into a single-lobed beam by using a binary diffractive optical
50 element playing the role of the rectifier [18].
- 51 • A simple diaphragm can transform a LG_1 beam into an optical bottle beam [19] or
52 a flat-top intensity profile [20].
53
54
55
56
57
58
59
60

1
2
3 lower-loss digitally controlled amplitude mask 3
4

5 2. Radial-order Laguerre-Gaussian modes intensity

6
7 Since the propagation of the Gaussian beam is well-known and can be derived
8 analytically [21], one can be able to transfer the understanding to higher-order modes.
9 Radial Laguerre-Gaussian (LG_p) beams have an intensity distribution that is made up
10 of the central bright lobe and concentric rings, thus the mathematical representation
11 can be written as shown in Eq. 1.
12

$$13 I = \frac{2}{\pi} \times \frac{1}{w_p^2} \times \left[L_p^0 \left(\frac{2r^2}{w_p^2} \right) \right]^2 \times e^{-\frac{2r^2}{w_p^2}}, \quad (1)$$

14
15 where r is the radial coordinates and L_p^0 is the Laguerre polynomial. All other
16 parameters have their usual meaning defined for Gaussian beams [22].
17

18 The maximum intensity occurs at central peak while the intensity associated with
19 the ring is lower. The radial intensity distribution of LG_p beams becomes broader as
20 mode order p increases and be characterised by a width (w_p) based on the second-
21 moment of the intensity pattern and the width (w_p) is given by:
22

$$23 w_p = w_0 \sqrt{2p + 1}, \quad (2)$$

24 where w_0 is the width of the Gaussian beam. In addition to Eq. 2, the propagation
25 property of LG_p beams is the propagation factor (M_p^2) that is defined by as:
26

$$27 M_p^2 = 2p + 1, \quad (3)$$

28 the propagation factor (M_p^2) is used to measure the beam quality of the laser beam
29 according to ISO Standard 11146 [23]. We can numerically analyse LG_p propagation by
30 starting with Laguerre Polynomial part of Eq. 1, taking radial-order $p = 1 - 4$. The
31 Laguerre polynomial and r_i the position of the zeroes of intensity are given in Tab. 1
32 of Ref. [12]. To force the laser to generate LG_p modes, a digital mask containing p -
33 absorbing rings that have a geometry which closely follows the location of the Laguerre
34 polynomial p -zeros as illustrated in Tab. 2 of Ref. [12], were digitally encoded and
35 displayed on to intra-cavity SLM screen of the laser resonator [11], which then allowed
36 for the generation of LG_p modes.
37

38 3. Experimental Methodology and Concept

39 We considered a planoconcave solid-state laser (DPSSL) resonator that is diode-pumped
40 with a multi-mode fibre coupled diode laser, for the generation of radial order Laguerre-
41 Gaussian (LG_p) modes. The Hamamatsu spatial light modulator (X10468-03) was
42 encoded with an amplitude mask that operates as an end mirror of the solid-state
43 digital laser [11]. The amplitude mask was encoded to have p -absorbing rings of varying
44 width thickness that will nearly 98% match each null of the LG_p mode, and varying the
45 completeness of the ring for radial-order $p = 1 - 4$. A schematic of the experimental
46 setup is presented in Fig. 1.
47

48 The gain medium is a Nd: YAG rod crystal of 25 mm in length with a 1.1%
49 neodymium concentration, and it was pumped with a diode laser operating at 808 nm.
50
51
52
53
54
55
56
57
58
59
60

lower-loss digitally controlled amplitude mask

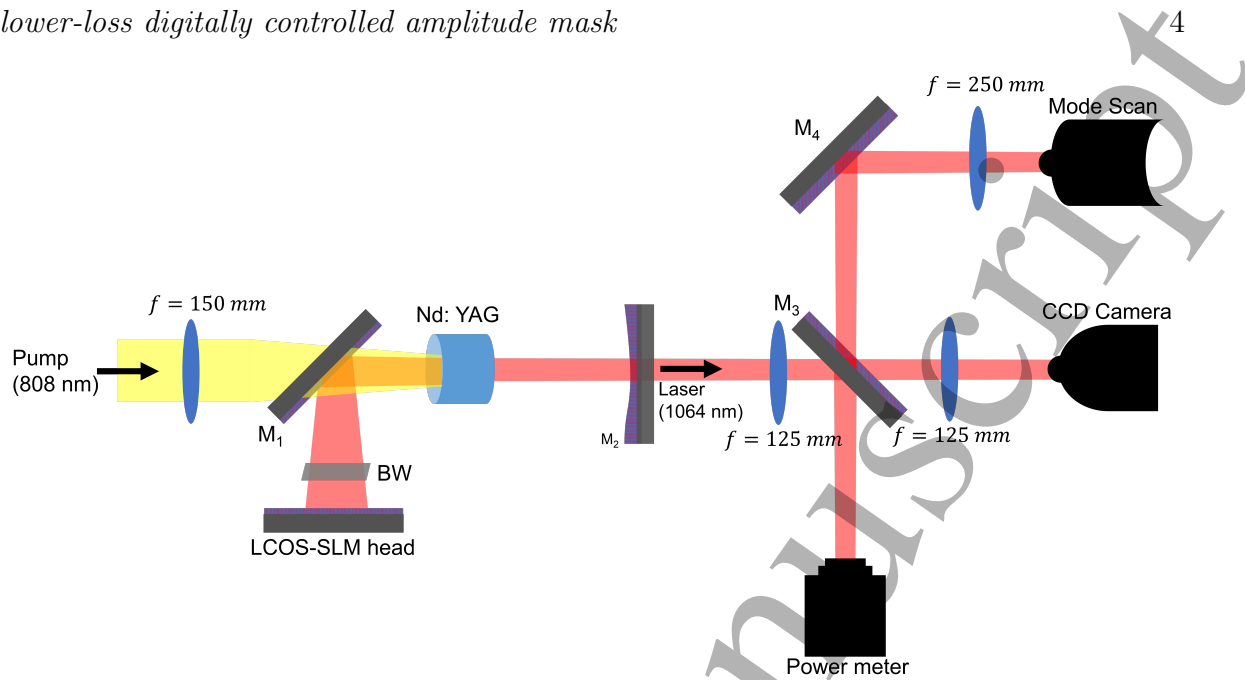


Figure 1. Schematic of a diode-pumped solid-state digital laser. The laser beam was transmitted out of the cavity through an output coupler mirror (M_2), and was 1:1 relay imaged using two lenses with focal length of 125 mm to the USBeamPro CCD Camera. In addition, the transmitted beam was relay imaged and expanded using two lenses with focal length 125 mm and 250 mm, respectively, to a ModeScan for measuring the beam quality factor M_p^2 . Mirror M_3 is used as a flip and twist mirror that allows one to transmit the beam to the CCD or ModeScan or Power meter.

The laser crystal was mounted inside a 21 °C water-cooled copper block. The diode laser pump (Jenoptic, JOLD-75-CPXF-2P) have a maximum output power of 75 Watts at an emission wavelength of 808 nm (at an operating temperature of 25 °C). A gain area with a radius of 2 mm was then excited within the centre of the Nd: YAG rod crystal by a focusing (by a lens with 150 mm focal length) the pump beam.

The planoconcave resonator cavity is comprised of a phase-only SLM which acted as a plane end mirror of the cavity with a reflectivity of 95% and a curved output coupler mirror (M_2) with a radius of curvature of 400 mm and a reflectivity of 90%. Since the SLM is a phase-only device, yet many of the desired holograms require both amplitude and phase change to the field. In order to achieve this, we make use of the well-known methods of complex amplitude modulation [24, 25], because this is suitable for implementation on the SLMs. Between the SLM and the mirror (M_1), the brewster window, (BW), was used to force the polarisation of the laser to match the eigen polarisations of the SLM.

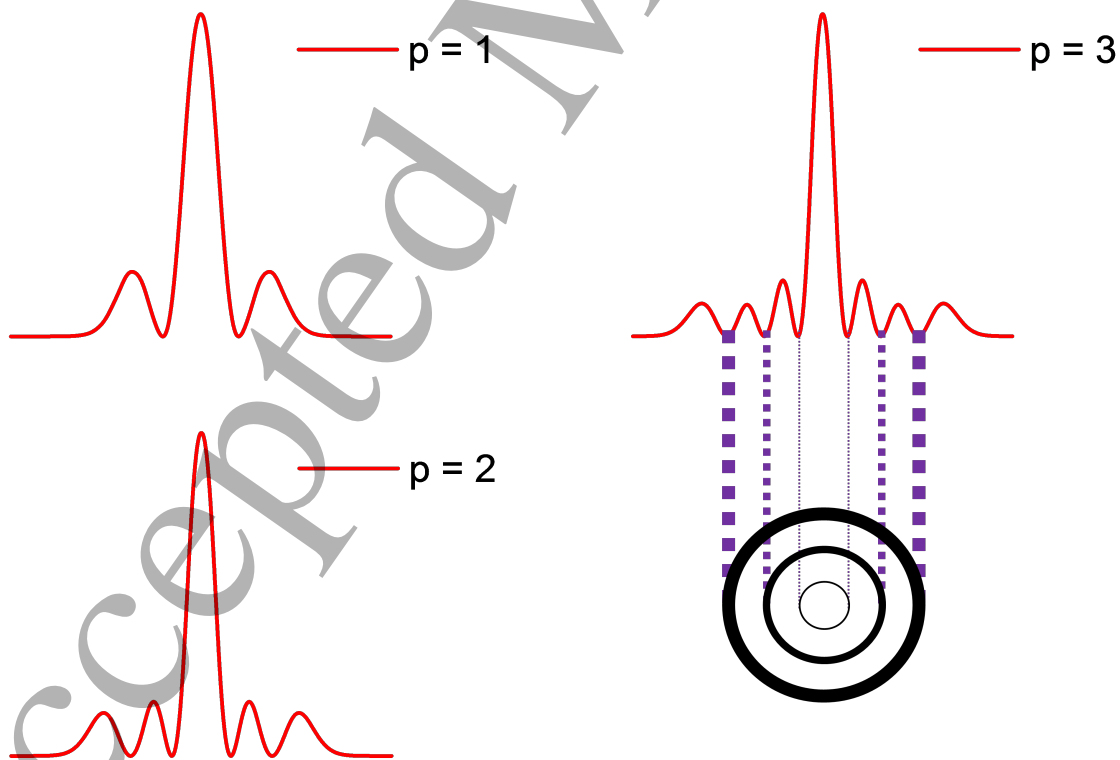
The resonator was designed to form an L-shape (in order to avoid illuminating the SLM with the residual pump light) by including a 45° mirrors (M_1) within the cavity that was highly reflective for 1064 nm and highly transmissive for 808 nm. The resonator length was chosen to be 160 mm. The laser beam was transmitted out of the cavity through an output coupler mirror (M_2), and was 1:1 relay imaged using two lenses to the

1
2
3 *lower-loss digitally controlled amplitude mask* 5

4
5 USBeamPro CCD Camera Beam Profiler (Photon Inc.). The CCD camera was used to
6 capture images that are normalised to 1 and was also used to measure the beam width.
7 In addition, the transmitted beam was relay imaged and expanded to a ModeScan-1780
8 Laser M^2 Measuring System (Ophir Photonics) for measuring the beam quality factor
9 M_p^2 . The power meter is used measure the output power of the laser.
10
11

12 13 4. Numerical simulations for complete ring

14
15 We performed a numerical calculation of the fundamental mode of the resonator that
16 will contain an intra-cavity amplitude mask that will match an appropriate ring mask.
17 The simulation is based on the expansion of the resonant field on the basis of the
18 eigenmodes of the bare cavity (without any diffracting object). This method will not be
19 given here since it has been already described elsewhere for the case of a planoconcave
20 cavity including an absorbing ring on the plane mirror [26]. The simulation given in
21 Ref. [26] can be easily adapted to the case of an amplitude mask made up of concentric
22 absorbing rings just by evaluating the overlapping integral (Eq. A10 of Ref. [26]) upon
23 all the regions of transparency of the mask.
24
25
26
27
28
29
30



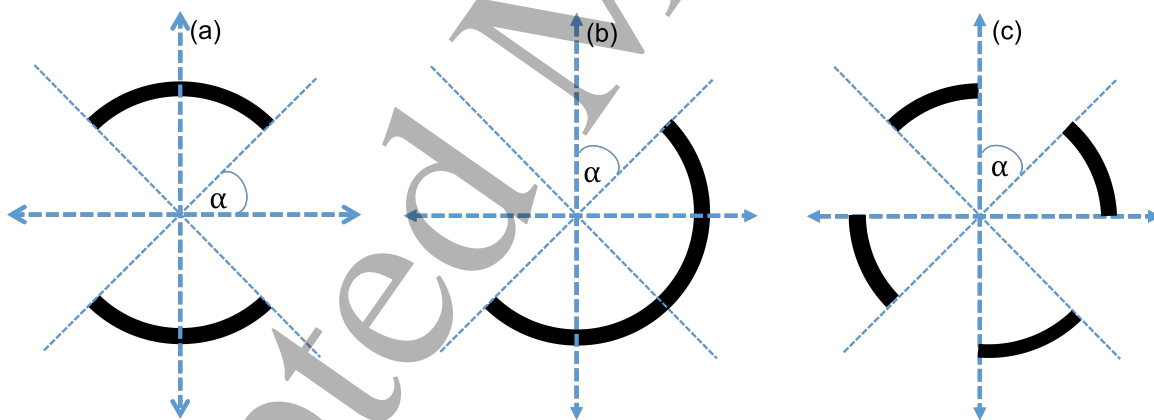
56
57
58 **Figure 2.** Intensity cross section of numerically simulated lowest-loss eigenmodes
59 for $p = 1$ to 3, when a mask containing an absorbing p -rings is inserted inside the
60 resonator. The mask is inserted such that the high-loss absorbing rings coincide with
the intensity p -zero nulls for an example for $p = 3$, LG_p mode.

1
2
3 lower-loss digitally controlled amplitude mask 6
4

5 The width thickness of absorbing rings is designed to be 98% the theoretical width
6 thickness the LG_p mode p -zero nulls that will be oscillating inside the resonator (Fig. 1).
7 The simulated LG_p modes of $p = 1 - 3$ cross-section profiles are shown in Fig. 2. The
8 width thickness of the p -absorbing rings for $p = 3$ mode, increases from the inner ring
9 to the outer ring. The minimum width thickness of the ring is $20 \mu\text{m}$ which corresponds
10 to the pixel pitch of the SLM. It is worthwhile to note that the fundamental mode of
11 the laser cavity is the mode reaching first the oscillation threshold and which is not
12 Gaussian in shape in the presence of the mask. The fundamental mode is an LG_p with
13 p adjustable from $p = 1$ to 3 depending on the number of absorbing rings making up
14 the mask.
15
16
17
18
19

20 5. Numerical simulations for incomplete ring

21 From Sec. 3, the planoconcave cavity has been shown to have a length $L = 160$ mm, and
22 the concave mirror (M_2) have a radius of curvature $R = 400$ mm. Now, we will focus on
23 the generation of an LG_p mode imposed by the insertion of a single absorbing ring of
24 radius r_A . The ring is set against the plane mirror (SLM of Fig. 1) and a diaphragm of
25 radius r_0 is set against the plane mirror (SLM of Fig. 1). For our case, the p -absorbing
26
27
28
29
30



46 **Figure 3.** Schematic diagram illustrating a 50% complete p -absorbing ring, regardless
47 of the symmetry. With α representing the incompleteness of the ring.
48

49 ring diaphragm was encoded to the SLM. Part of the fundamental mode loss level is
50 due to the circular absorbing ring mask, and we expect to reduce the losses by using an
51 incomplete absorbing ring mask shown in Fig. 3.
52

53 The losses associated with the incompleteness of the absorbing ring does not depend
54 on how many times the absorbing ring has been segmented as shown in fig. 3. The losses
55 of the laser depend on the overall effect of each incomplete absorbing ring. i.e. For a full
56 ring, $\alpha = 0$, the fundamental mode of the resonator is expected to be Laguerre-Gaussian
57 mode of radial order $p = 1$ (LG_1), with a beam propagation factor $M^2 = 3$ (by choosing
58 $p = 1$ and $l = 0$ in Eq. 3).
59
60

lower-loss digitally controlled amplitude mask

7

The ring is almost non-existent, at $\alpha > 0.95\pi/2$, thus the Gaussian mode will oscillate. However, the LG_p of order $p=1$ will oscillate provided that the angle α of the absorbing ring is kept less than $0.95\pi/2$ as shown in Fig. 4a. The propagation factor M^2 of the fundamental mode remains equal to 3 as shown in Fig. 4b, up until the angle α is close to $\pi/2$ when the laser resonator will then select $p=0$ mode and the M^2 will then become 1. The losses of the fundamental mode, δ , are indicated in Fig. 5a,

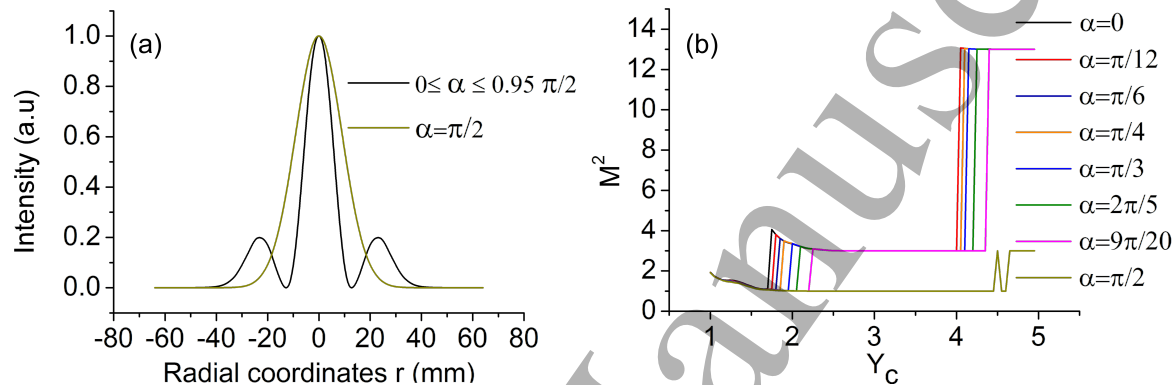


Figure 4. (a) Numerically simulated fundamental mode shape at the far-field. (b) Numerically simulated propagation factor M^2 as a function of truncation ratio Y_C .

as a function of the beam truncation ratio Y_C for different values of angle α . When $\alpha = \pi/2$, the cavity is expected to generate a Gaussian fundamental mode of $p = 0$, since the cavity losses will be the lowest as shown in Fig. 5a. When $\alpha = 0$, the cavity is expected to generate a $p = 1$ as the fundamental mode of the cavity since the ring will be complete and the losses will be the highest. The simulation of the losses of the laser

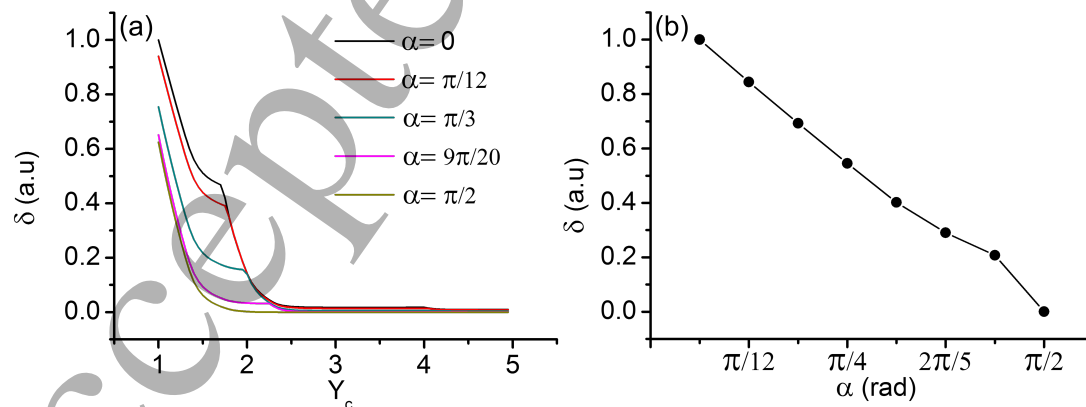


Figure 5. (a) Numerically simulated intra-cavity losses, δ , of the fundamental mode as the function of the beam truncation ratio, (Y_C). (b) Numerically simulated intra-cavity losses, δ , of the fundamental mode as the function of ring incompleteness (α).

resonator as a function of the absorbing ring incompleteness angle, α , is shown in Fig.

1
2
3
4
5
6
7
8
9
10
11
12
13
14
15
16
17
18
19
20
21
22
23
24
25
26
27
28
29
30
31
32
33
34
35
36
37
38
39
40
41
42
43
44
45
46
47
48
49
50
51
52
53
54
55
56
57
58
59
60

lower-loss digitally controlled amplitude mask 8

5b. The simulation shows that varying angle, α , from a full ring of 100% completeness of $\alpha = 0$ to $\alpha = 9\pi/20$, the cavity will select $p = 1$ mode as the fundamental mode of the cavity; and between $\alpha = 9\pi/20$ and $\alpha = \pi/2$, the simulation shows that the losses will be decreasing at a fast rate towards zero and the laser resonator will then select the $p = 0$ as the Gaussian fundamental mode. The concept is tested by varying of completeness of the ring, by varying α on the CGDH. The experimental results are shown in Sec. 6, where we measured the pumping threshold, ϵ_{th} , the propagation factor, M_p^2 , the generated LG_{*p*} beam width, w_p , and the slope efficiency, η_p , of the output LG_{*p*} beams.

6. Experimental Results and Discussion

The intensity distributions profiles results for selected laser modes with the varying completeness of the p -absorbing ring are shown in Fig. 6. The absorbing ring completeness was varied from 12.5% to 100%. The method used to excite the modes from the cavity was by employing CGDH amplitude masks which were encoded as pixelated grey images and displayed onto an SLM that also acted as a flat end mirror of the resonator of the diode end-pumped solid-state laser (DPSSL) resonator [11]. The CGDH amplitude masks contained p -absorbing rings of varying circular completeness and their corresponding intensity profiles are shown in Fig. 6a, 6b, 6c and 6d, for LG_{*p*} mode of order $p = 1$ to 4, respectively.

The results in Fig. 7a shows that when the completeness of the ring is less than 37.5%, the cavity is not generating LG_{*p*} mode but different laser beams with varying propagation factor, M^2 values. The results further confirm that when the completeness of the ring is greater or equal to 37.5%, the resonator produces the expected LG_{*p*} modes with a propagation factor M^2 values close to $(2p+1)$ the theoretical values given by Eq. 3, for all generated LG_{*p*} modes from $p = 1$ to $p = 4$. Therefore our stable resonator cavity conforms to the ABCD matrix [17] theory when the completeness of the ring is greater and equal to 37.5% as shown by the results in Fig. 7b; where the generated LG_{*p*} mode width, w_p , follow closely the theory given in Eq. 2.

Since the output power from the laser resonator is defined to be linearly proportional to the mode volume, V_p , where the volume of the p^{th} radial mode is given as:

$$V_p = V_0 M^2 \left(1 + \frac{l_0^2}{3z_r^2} \right), \quad (4)$$

where l_0 is the length of the gain medium and V_0 is the mode volume of the Gaussian mode. From Eq. 4 it is clear that the mode volume, V_p , is directly proportional to the propagation factor, M^2 , of the fundamental LG_{*p*} mode; and therefore we can deduce that the output power extracted from the laser is also directly proportional to both the mode volume, V_p , and the propagation factor, M^2 , of the oscillating LG_{*p*} mode [27]. The experimental results shown in Fig. 8a suggest that the mask with a completeness comprised between 37.5% to 100% is able to select an LG_{*p*} mode, as proven by the slope efficiency of the laser to be constant for each LG_{*p*} laser mode. Furthermore, the

lower-loss digitally controlled amplitude mask

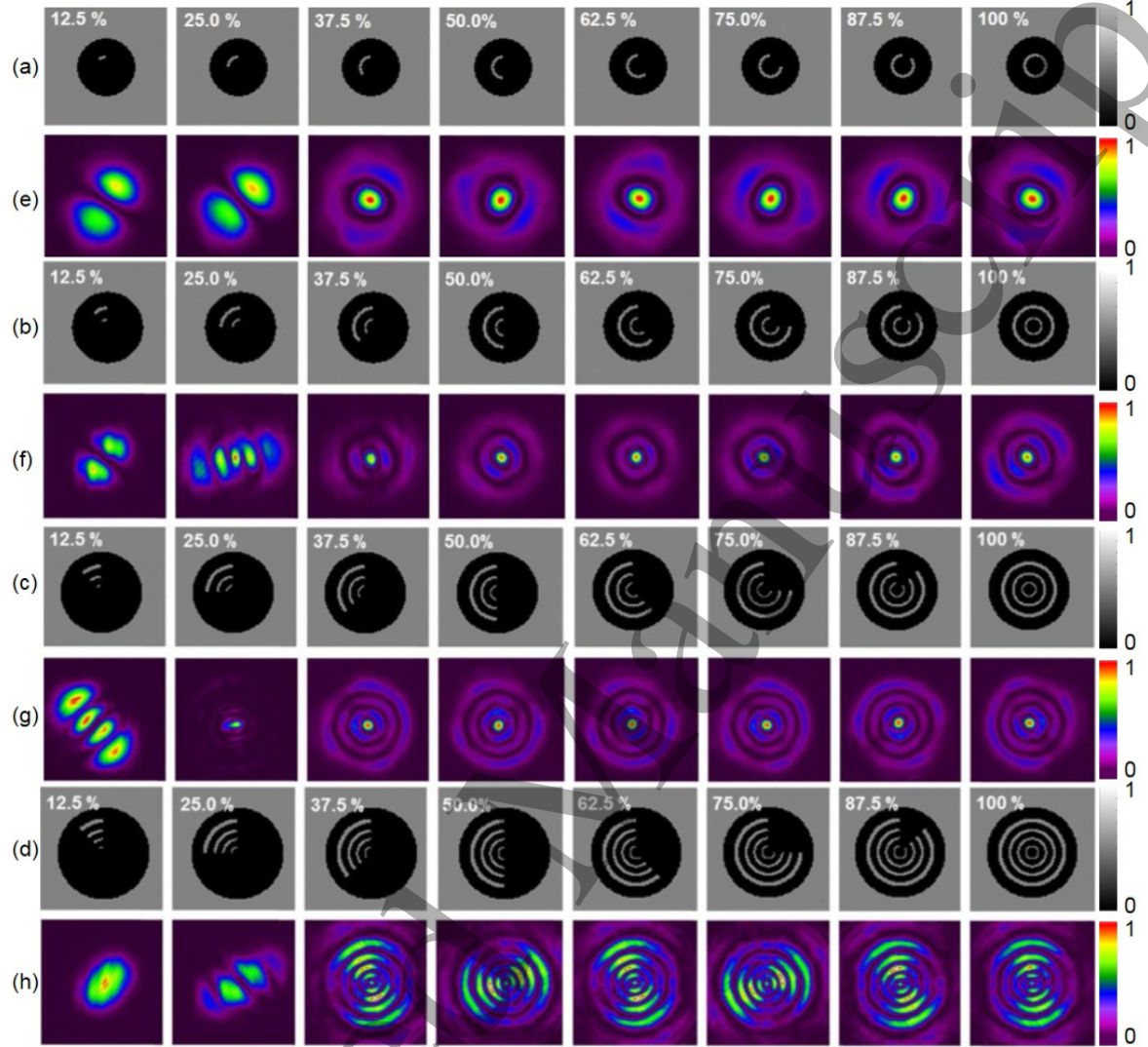


Figure 6. The top row of (a)-(d) shows computer generated digital holograms encoded as pixelated greyscale (0 to 1) images on the SLM where the completeness of the p -absorbing ring is varied. Bottom rows of (e)-(h) show the generated intensity profiles (normalised to 1) from the laser output coupler mirror for the different corresponding p -absorbing ring digital holograms on the SLM.

threshold of the laser resonator with respect to the pump power, P_ϵ , and the absorbed pump power, $P_{abs,\epsilon}$, can be mathematically described as follow [15]:

$$P_\epsilon = \frac{\pi h \nu_\epsilon}{4 \eta_{(\epsilon-q)} \sigma_{em} \tau} (w_p^2 + w_\epsilon^2) (T + L) \quad \text{and}; \quad (5)$$

$$P_{abs,\epsilon} = \eta_{(\epsilon-q)} \frac{\nu_l T + L}{\nu_\epsilon T}, \quad \text{for } w_\epsilon < w_p, \quad (6)$$

where w_p and w_ϵ are the laser LG_p mode radius and pump radius; ν_l and ν_ϵ are the laser and pump frequencies; σ_{em} is the effective stimulated-emission cross-section; τ is the lifetime of the laser transition; $\eta_{(\epsilon-q)}$ is the pump quantum efficiency which is the

lower-loss digitally controlled amplitude mask

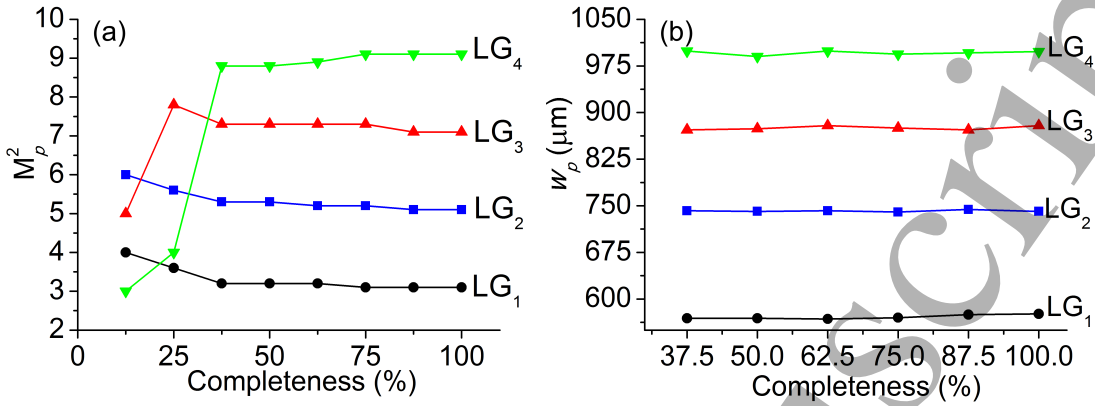


Figure 7. (a) Beam propagation factor, M_p^2 , and (b) beam radius, w_p , at the output coupler for LG modes of $p = 1 - 4$ with varying completeness of the absorbing rings.

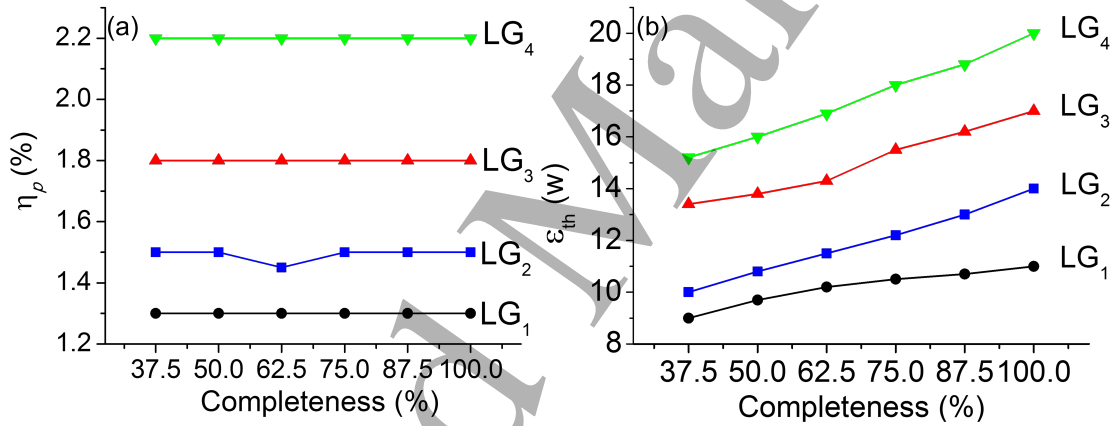


Figure 8. The graphs showing the slope efficiency, (a) η_p , and the pump power threshold, (b) ϵ_{th} , for LG _{p} modes of $p = 1 - 4$ with varying completeness of the absorbing circular ring.

average number of ions in the upper manifold created per absorbed pump photon; T is the output coupler transmission and L is the laser resonator losses, such as scattering, absorbing rings, aberrations due to thermal effects. The only major resonator loss, L , that we are interested is to study the laser resonator absorbing rings. Since the slope efficiency, η_p , of the laser resonator for each LG _{p} mode generated is given as:

$$\eta_p = \eta_{(\epsilon-q)} \frac{\nu_l}{\nu_\epsilon}. \quad (7)$$

Using Eq. 6, then η_p can be represented as:

$$\eta_p = P_{abs,\epsilon} \frac{T}{T + L}. \quad (8)$$

It is important to note that Eq. 5 and Eq. 6 are only valid for $T \ll 1$ and $L \ll 1$, otherwise T must be replaced with $-\ln(1 - T)$, and $L = \sum L_i$, where L_i are all the separate cavity losses other than the output coupler, which in our case it will be

1
2
3 *lower-loss digitally controlled amplitude mask* 11

4 absorbing rings losses, δ , for each LG_p mode. However, up to few percent loss, the
5 transmission approximations are very good ($-\ln(1 - T) = 0.051$ for $T = 0.050$ and
6 $-\ln(1 - T) = 0.105$ for $T = 0.100$). Therefore inserting Eq. 8 into Eq. 5 and Eq. 6,
7 and solving for slope efficiency, η_p , the equation will become:
8

$$9 \quad \eta_p = \frac{\pi h \nu_l}{4 \sigma_{em} \tau} \times \frac{(w_p^2 + w_\epsilon^2)}{P_\epsilon} \times (T + L). \quad (9)$$

10 From Eq. 9, it is also clear that the slope efficiency, η_p , is directly proportional to
11 the LG_p mode volume, V_p , since the absorbing ring losses L and the pump power, P_ϵ ,
12 cancel each other for each LG_p amplitude mask as they always simultaneously increase
13 concurrent. This effectively makes the slope efficiency, η_p , to be constant as shown in
14 Fig. 8a for various ring completeness, from ring completeness equal or greater than \approx
15 37.5%, when the laser resonator is generating LG_p modes.
16

17 It is observed in Fig. 8b that the pump threshold, ϵ_{th} is shown to increases linearly
18 as the absorbing rings completeness or losses increases, for each LG_p mode. The lowest
19 pump threshold, ϵ_{th} , for the generation of LG_p modes is shown to occur when the
20 completeness of the absorbing rings is at $\approx 37.5\%$ and this is $\approx 2\pi/5$ shown by Fig. 8b.
21 These results are 93% ($(2\pi/5)/(9\pi/20)$) in good agreement with the simulation shown
22 in Fig. 5b where the simulation shows that the laser starts operating on high LG_p mode
23 when $\alpha > 9\pi/20$.
24
25
26
27
28
29
30
31

32 7. Conclusion

33 Forcing the fundamental mode of a laser to be an LG_p mode, can be obtained by
34 inserting a mask made up of p -absorbing rings having radii coinciding with the zeros of
35 the desired radial Laguerre-Gaussian mode. However, doing that increases the loss level
36 and the laser threshold. In this work, we have experimentally demonstrated that it is
37 possible to reduce the additional losses by using a mask having a completeness equal
38 or greater than 37.5%. The better results in terms of the laser threshold are obtained
39 for a completeness of 37.5%. We have successfully demonstrated that high-radial-order
40 Laguerre-Gaussian, LG_p , modes can be generated using circular absorbing rings that
41 are $\approx 37.5\%$ to 100% complete. The results also indicate that we can digitally excite
42 high-radial-order LG_p modes with the lowest excitation pump threshold, ϵ_{th} , when the
43 absorbing rings are $\approx 37.5\%$ complete or when $\alpha = 2\pi/5$, while maintaining all the
44 other resonator characteristics (such as the generated LG_p mode size, w_p , beam quality
45 factor, M_p^2 , and the slope efficiency, η_p , of the laser).
46
47
48
49
50
51
52
53

54 Funding Information

55 Department of Science & Technology (DST) and National Research Foundation
56 (NRF)(86104:2015); The Professional Development Programme Doctoral Block Grant.
57
58
59
60

1
2
3 lower-loss digitally controlled amplitude mask 12
4

5 Acknowledgements

6
7 We thank the CSIR-National Laser Centre (South Africa) and University of KwaZulu-
8 Natal School of Chemistry and Physics (Dr M.K. Moodley) for their support.
9

10 References

- 11
12
13 [1] K. Sueda, G. Miyaji, N. Miyanaga, and M. Nakatsuka, "Laguerre-Gaussian beam generated with a
14 multilevel spiral phase plate for high intensity laser pulses," *Opt. Express*, vol. 12, pp. 3548–3553,
15 2004.
16
17 [2] N. Matsumoto, T. Ando, T. Inoue, Y. Ohtake, N. Fukuchi, and T. Hara, "Generation of
18 high-quality higher-order Laguerre-Gaussian beams using liquid-crystal-on-silicon spatial light
19 modulators," *JOSA A*, vol. 25, pp. 1642–1651, 2008.
20
21 [3] D. Rhodes, D. Gherardi, J. Livesey, D. McGloin, H. Melville, T. Freegarde, and K. Dholakia, "Atom
22 guiding along high order Laguerre-Gaussian light beams formed by spatial light modulation,"
23 *J. Mod. Opt.*, vol. 53, pp. 547–556, 2006.
24
25 [4] A. Mair, A. Vaziri, G. Weihs, and A. Zeilinger, "Entanglement of the orbital angular momentum
26 states of photons," *Nat*, vol. 412, pp. 313–316, 2001.
27
28 [5] K. C. Neuman and S. M. Block, "Optical trapping," *Review of scientific instruments*, vol. 75,
29 pp. 2787–2809, 2004.
30
31 [6] F. Pampaloni and J. Enderlein, "Gaussian, Hermite-Gaussian, and Laguerre-Gaussian beams: A
32 primer," *arXiv*, 2004.
33
34 [7] N. Simpson, L. Allen, and M. Padgett, "Optical tweezers and optical spanners with Laguerre-
35 Gaussian modes," *J. Mod. Opt.*, vol. 43, pp. 2485–2491, 1996.
36
37 [8] T. Godin, S. Ngcobo, E. Cagniot, M. Fromager, A. Forbes, and K. Aït-Ameur, "Strong reducing
38 of the laser focal volume," in *SPIE Optical Engineering+ Applications*, pp. 81300Q–81300Q,
39 International Society for Optics and Photonics, 2011.
40
41 [9] J. Arlt, R. Kuhn, and K. Dholakia, "Spatial transformation of Laguerre-Gaussian laser modes,"
42 *J. Mod. Opt.*, vol. 48, pp. 783–787, 2001.
43
44 [10] Y.-X. Ren, M. Li, K. Huang, J.-G. Wu, H.-F. Gao, Z.-Q. Wang, and Y.-M. Li, "Experimental
45 generation of Laguerre-Gaussian beam using digital micromirror device," *Appl. Opt.*, vol. 49,
46 pp. 1838–1844, 2010.
47
48 [11] S. Ngcobo, I. Litvin, L. Burger, and A. Forbes, "A digital laser for on-demand laser modes," *Nat*,
49 vol. 4, 2013.
50
51 [12] S. Ngcobo, K. Aït-Ameur, N. Passilly, A. Hasnaoui, and A. Forbes, "Exciting higher-order radial
52 Laguerre-Gaussian modes in a diode-pumped solid-state laser resonator," *Appl. Opt.*, vol. 52,
53 pp. 2093–2101, 2013.
54
55 [13] S. Ngcobo, T. Bell, K. Ait-Ameur, and A. Forbes, "Low-loss selective excitation of higher-order
56 modes in a diode-pumped solid-state digital laser," in *SPIE Optical Engineering+ Applications*,
57 pp. 95810S–95810S, International Society for Optics and Photonics, 2015.
58
59 [14] T. Bell, A. Hasnaoui, K. Aït-Ameur, A. Forbes, and S. Ngcobo, "Intracavity generation of low-loss
60 radial-order Laguerre-Gaussian modes using digital holograms," in *SPIE LASE*, pp. 97271K–
97271K, International Society for Optics and Photonics, 2016.
[15] T. Y. Fan and R. L. Byer, "Diode laser-pumped solid-state lasers," *IEEEJ. Quant. Electron*, vol. 24,
pp. 895–912, 1988.
[16] S. Kubota and Y. Kaneda, "End pumped solid-state laser," Apr. 13 1993. US Patent 5,202,893.
[17] W. Koechner, *Solid-state laser engineering*, vol. 1. Springer, 2013.
[18] A. Hasnaoui, A. Bencheikh, M. Fromager, E. Cagniot, and K. Aït-Ameur, "Creation of a sharper
focus by using a rectified tem p0 beam," *Optics Communications*, vol. 284, no. 5, pp. 1331–1334,
2011.

lower-loss digitally controlled amplitude mask

13

- [19] A. Hasnaoui, S. Haddadi, M. Fromager, D. Louhibi, A. Harfouche, E. Cagniot, and K. Ait-Ameur, "Transformation of a lg10 beam into an optical bottle beam," *Laser Physics*, vol. 25, no. 8, p. 085004, 2015.
- [20] S. Haddadi, A. Hasnaoui, M. Fromager, D. Louhibi, A. Harfouche, E. Cagniot, and K. Ait-Ameur, "Use of a diaphragm for transforming a lg 10 beam into a flat-top," *Optik-International Journal for Light and Electron Optics*, vol. 127, no. 4, pp. 2207–2211, 2016.
- [21] J. Alda, "Laser and gaussian beam propagation and transformation," *Encyclopedia of Optical Engineering*, vol. 2013, pp. 999–1013, 2003.
- [22] H. Kogelnik and T. Li, "Laser beams and resonators," *Applied optics*, vol. 5, no. 10, pp. 1550–1567, 1966.
- [23] Standard, "Lasers and laser-related equipment-test methods for laser beam widths, divergence angles and beam propagation ratios," *ISO*, 2005.
- [24] V. Arrizón, U. Ruiz, R. Carrada, and L. A. González, "Pixelated phase computer holograms for the accurate encoding of scalar complex fields," *JOSA A*, vol. 24, no. 11, pp. 3500–3507, 2007.
- [25] V. Arrizón, "Optimum on-axis computer-generated hologram encoded into low-resolution phase-modulation devices," *Optics letters*, vol. 28, no. 24, pp. 2521–2523, 2003.
- [26] A. Hasnaoui and K. Ait-Ameur, "Properties of a laser cavity containing an absorbing ring," *Appl. Opt*, vol. 49, pp. 4034–4043, 2010.
- [27] T. Bell and S. Ngcobo, "Selective excitation of higher-radial-order laguerre-gaussian beams using a solid-state digital laser," *J Laser Opt Photonics*, vol. 3:144, 2017.